The Effects of Compression Forces on the Crowd Dynamics

Guillermo A. Frank* Ignacio M. Sticco† Claudio O. Dorso‡

Abstract

The collective dynamics of pedestrians display complex phenomena involving slowings down due to clogging, and even, turbulent patterns. Casualties may occur, although these can be (partially) anticipated by performing computer simulations. The Social Force Model (SFM) has been shown to be suitable for describing the crowd behavior. In its present version, the parameters of the model are not well determined experimentally. So, in order to perform more realistic simulations some of these parameters should be critically reviewed. In this communication we specifically investigated the effects of the stiffness parameter (which describes the compressibility of the pedestrian's body)on the crowd dynamics. We analyzed the corresponding simulations for the evacuation of corridors and bottlenecks. Our main conclusion is that mutual coordination between the individual's stiffness and the geometrical configuration is required for attaining an enhanced evacuation efficiency.

Key Words: Collective dynamics, Social Force Model, body stiffness

1. Introduction

In its original version, the SFM, addresses two physical forces as essential: the "body force" and the "sliding friction". Both are inspired by granular interactions and were claimed to be necessary for attaining the particular effects in panicking crowds [1]. The "sliding friction" actually proved to be an essential feature of the "faster-is-slower" effect, although the role of the "body force" appears, at a first instance, not so clear [2, 3, 4].

Researchers, however, question the numerical setting for the "body force" in the SFM context [5]. As a matter of fact, the usual set of parameters provided by Helbing prevents the excessive overlapping among pedestrians, but it is known to accomplish artificially high force levels [1, 5, 6, 7]. The empirical fundamental diagram raises as a point of reference for the realistic estimation of the SFM control parameters [8, 9].

The fundamental diagram exhibits the flux behavior for either low density crowds (with rare contacts between pedestrians) and highly dense crowds

*Unidad de Investigación y Desarrollo de las Ingenierías, Universidad Tecnológica Nacional, Facultad Regional Buenos Aires, Av. Medrano 951, 1179 Buenos Aires, Argentina

†Departamento de Física, Facultad de Ciencias Exactas y Naturales, Universidad de Buenos Aires, Pabellón I, Ciudad Universitaria, 1428 Buenos Aires, Argentina

‡Instituto de Física de Buenos Aires, Pabellón I, Ciudad Universitaria, 1428 Buenos Aires, Argentina.

(dominated by two body interactions). In the second case, crowds experience a flux slowing down, but other behaviors are also possible [8, 10]. We may suspect that the modeling of the "flux slowing down" within the context of the SFM will require the proper setting of the controlling parameters. In this paper, we will explore the complex interplay between the body force and the sliding friction among pedestrians.

The paper is organized as follows. We first recall the available experimental values on the body force and the sliding friction (see Section 2). We present our numerical simulations in Section 4. For the sake of clarity, this Section is separated into three major parts: the bottleneck scenario, the corridor scenario and the comparison with empirical data in Sections: 4.1, 4.2 and 4.3, respectively. Section 5 opens a detailed discussion from results in Section 4 and resumes our main conclusions.

2. Experimental background

The moving patterns of the pedestrians are commonly quantified in the literature into the following characteristic parameters.

(i) The walking attitude of a pedestrian is related to his (her) reaction to unexpected behaviors [5, 11]. The associated parameter to this behavior is the relaxation or characteristic time τ [12, 1].

(ii) The desired speed v_d expresses his (her) motivation or intention to reach a certain destination (as comfortable as possible). Observations commonly associate $0.6\,\mathrm{m/s}$, $1\,\mathrm{m/s}$ or $1.5\,\mathrm{m/s}$ to relaxed, normal or nervous walking speeds, respectively [11, 1, 13].

(iii) Pedestrians tend to reduce their speed within crowded environments because they perceive not enough space for taking a step [12]. This (perceived) step distance known as the characteristic length B.

(iv) The "body force" and "sliding friction" can be introduced straight forward (see Section 3). But it is worth noting that both are associated to the moving difficulties (say, slowing down and obstructions) observed in contacting pedestrians.

Table 1 shows a few empirical values for the most common parameters. More data is available throughout the literature (see, for example, Refs. [14, 15, 16, 17, 18, 19, 13]). We intentionally omitted data that assumes a specific mathematical model.

The maximum (realistic) overlap may be computed from the Hooke's relation $F(x) = k_n(x)\,x$ and the compressibility $k_n(x)$ reported in Table 1. An "uncomfortable" body force $10\,\mathrm{N} - 30\,\mathrm{N}$ can address overlap values in the range of $0.030 - 0.055\,\mathrm{m}$. Also, a "hitting" force of $60\,\mathrm{N}$ can address overlap values between 0.045 and $0.065\,\mathrm{m}$. Besides, no reliable values for the sliding friction k_t appears to be available in the literature (to our knowledge).

τ[s]	m[kg]	v_d[m/s]	B[m]	k_n[kg/s^2]	Refs.
0.61	—	1.24	$0.36 + 1.06\,v$	—	[15]
0.50*	80*	1.34	0.50	—	[20, 5]
—	67.5	1.39	—	$96.1 + 12694.1\,x$	[21]
—	67.0	1.39	—	$97.0 + 29378.9\,x$	[21]

Table 1: The experimental data for the pedestrian parameters, as explained in Section 2. The magnitude v means the actual pedestrian velocity (m/s). The magnitude x means the compression length (m). The upper row for Ref. [21] corresponds to data acquired in winter and the lower row to data acquired in summer. The asterisk (*) corresponds to reasonable estimates from the authors.

3. Theoretical background

3.1 The Social Force Model

The Social Force Model (SFM) provides a necessary framework for simulating the collective dynamics of pedestrians (*i.e.* self-driven particles). The pedestrians are considered to follow an equation of motion involving either "socio-psychological" forces and physical forces (say, granular forces). The equation of motion for any pedestrian i (of mass m_i) reads

$$m_i \frac{d\mathbf{v}_i}{dt} = \mathbf{f}_d^{(i)} + \sum_{j=1}^{N} \mathbf{f}_s^{(ij)} + \sum_{j=1}^{N} \mathbf{f}_g^{(ij)} \tag{1}$$

where the subscript j corresponds to any neighboring pedestrian or the walls. The three forces $\mathbf{f}_d$, $\mathbf{f}_s$ and $\mathbf{f}_g$ are different in nature. The desire force $\mathbf{f}_d$ represents the acceleration (or deceleration) of the pedestrian due to his (her) own will. The social force $\mathbf{f}_s$, instead, describes the tendency of the pedestrians to stay away from each other. The granular force $\mathbf{f}_g$ stands for both the sliding friction and the compression between pedestrians.

The pedestrians' own will is modeled by the desire force $\mathbf{f}_d$. This force stands for the acceleration (deceleration) required to move at the desired walking speed v_d. As mentioned in Section 2, this involves the reaction time τ. Thus, the desire force is modeled as follows

$$\mathbf{f}_d^{(i)} = m\,\frac{v_d^{(i)}\,\hat{\mathbf{e}}_d^{(i)}(t) - \mathbf{v}^{(i)}(t)}{\tau} \tag{2}$$

where $\hat{\mathbf{e}}(t)$ represents the unit vector pointing to the target position. $\mathbf{v}(t)$ stands for the pedestrian velocity at time t.

The tendency of any individual to preserve his (her) "private sphere" is accomplished by the social force $\mathbf{f}_s$. The model for this kind of "socio-psychological" behavior is as follows

$$\mathbf{f}_s^{(i)} = A\,e^{(R_{ij}-r_{ij})/B}\,\hat{\mathbf{n}}_{ij} \tag{3}$$

where r_{ij} means the distance between the center of mass of the pedestrians i and j, and $R_{ij} = R_i + R_j$ is the sum of the pedestrians radius. The unit vector $\hat{\mathbf{n}}_{ij}$ points from pedestrian j to pedestrian i, meaning a repulsive interaction.

The net distance (overlap) $|R_{ij} - r_{ij}|$ scales to the parameter B in the expression (3). This parameter plays the role of a fall-off length within the model, and thus, it may be somewhat connected to the (perceived) step distance mentioned in Section 2. Besides, the parameter A reflects the intensity of the social repulsion.

The granular force (say, the sliding friction plus the body force) reflects the moving difficulties encountered in very crowded environments. The expression for the granular force has been borrowed from the granular matter field, the mathematical expression reads as follows

$$\mathbf{f}_g^{(ij)} = k_t\, g(R_{ij} - r_{ij})\, (\Delta \mathbf{v}^{(ij)} \cdot \hat{\mathbf{t}}_{ij})\, \hat{\mathbf{t}}_{ij} + k_n\, g(R_{ij} - r_{ij})\ \hat{\mathbf{n}}_{ij} \tag{4}$$

where $g(R_{ij} - r_{ij})$ equals $R_{ij} - r_{ij}$ if $R_{ij} > r_{ij}$ and vanished otherwise. $\Delta \mathbf{v}^{(ij)} \cdot \hat{\mathbf{t}}_{ij}$ represents the relative tangential velocities of the sliding bodies (or between the individual and the walls).

3.2 Blocking clusters

A characteristic feature of pedestrian dynamics is the formation of clusters. Clusters of pedestrians can be defined as the set of individuals that for any member of the group (say, i) there exists at least another member belonging to the same group (j) in contact with the former. Thus, we define a "granular cluster" (C_g) es follows

$$C_g : P_i \,\epsilon\, C_g \Leftrightarrow \exists\ j \,\epsilon\, C_g / r_{ij} < (R_i + R_j) \tag{5}$$

where (P_i) indicate the *ith* pedestrian and R_i is his (her) radius (shoulder width). That means, C_g is a set of pedestrians that interact not only with the social force, but also with physical forces (*i.e.* friction force and body force). A "blocking cluster" is defined as the subset of clusterized particles (granular cluster) closest to the door whose first and last component particles are in contact with the walls at both sides of the door [2]. This clogging structure is responsible for worsening the evacuation performance.

3.3 Procedures

The implemented SFM parameters were the same as those in Ref. [1] (at the beginning of the exploratory procedure only). But the pedestrian's mass and radius were set to the more realistic values of 70 kg and 0.23 m, respectively. The force interactions between pedestrians were limited, however, to a cut-off distance of 0.88 m for attaining a *privacy sphere* that excludes second neighbors. The desired velcity was always set to 1 m/s in the corridor situation. Besides, the explored values of v_d for the bottleneck scenario ranged from

1 m/s to the extremely anxious situation of 10 m/s.

The Eq. (1) was numerically integrated by means of the velocity Verlet algorithm, with a timestep of 10^{-4} seconds. The pedestrians positions and velocities were recorded every 0.05 sec, but post-processing computing was done over samples acquired at least every 2 sec., in order to avoid data correlations. Those pedestrians leaving the simulations box were re-introduced into the box, on the opposite side (periodic boundary conditions). We only omitted this mechanism when computing the evacuation time for the bottleneck geometry.

We warn the reader that, for simplicity, we will not include the units corresponding to the numerical results. Remember that the friction coefficient has units $[k_t]$ =Kg m^{-1} s^{-1}, the body stiffness coefficient $[k_n]$ =Kg s^{-2}, the density $[\rho]$ =p m^{-2} and the flow $[J]$ =p m^{-1} s^{-1}.

4. Results

4.1 Bottleneck

We present in this section the results corresponding to the bottleneck geometry. We show the consequences of modifying the body force coefficient k_n on the evacuation dynamics. Recall that this coefficient is associated to the compression of the human body.

Fig. 1 shows the evacuation time as a function of the pedestrian's desired velocity for different values of k_n. Three behavioral patterns can be distinguished in Fig. 1. Each pattern can display a positive slope, a negative slope or both. The interval in which the slope is positive means that the harder the pedestrians try to get out (higher v_d), the longer it takes them to evacuate. This is the Faster- is-slower (FIS) regime. Conversely, the interval in which the slope is negative corresponds to a Faster-is-Faster (FIF) regime (the harder they try, the quicker they leave).

Fig. 1 shows either FIS or FIF, and a FIS+FIF pattern for desired velocities $v_d > 1.2$ m/s. The evacuation time attains a FIS+FIF pattern for compression coefficients below $k_n = 1.2$ E5. This means that "soft" individuals can attain this behavioral pattern. Notice that higher values of k_n allow only FIS or FIF patterns. For the highest explored value $k_n = 1.2$ E6, no FIS can be seen at all. Besides, the evacuation pattern for $k_n = 0$ and $k_n = 2.6$ E4 are very similar since the body force intensity is of the same order or less than the social force for these stiffness values.

Despite the presence of the FIS or FIF pattern, the evacuation time at a fixed value of v_d decreases for increasing values of k_n (within the examined interval). This means that stiffer pedestrians evacuate faster than soft pedes-

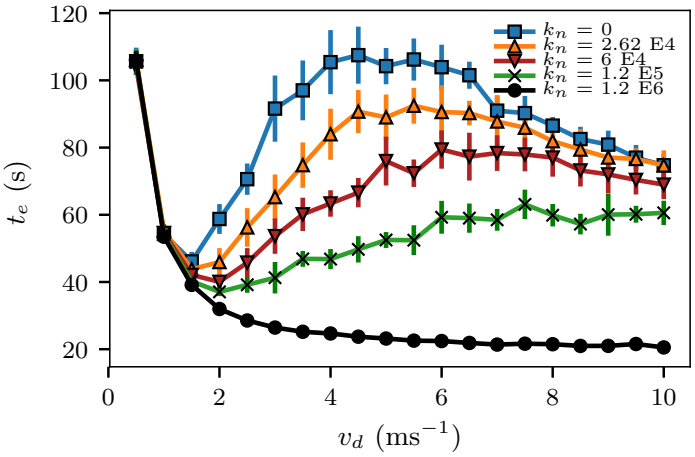

Figure 1: Mean evacuation time (s) vs. the pedestrians desired velocity (m/s) for a bottleneck. The room was 20 m x 20 m size. The door was 0.92 m width (two pedestrians' width). Mean values were computed from 10 evacuation processes. 225 pedestrians were initially placed in a square lattice with a random initial velocity. Each process was finished when 158 pedestrians left the room. The different symbols indicate the k_n value corresponding to the body force (see the label). The crosses correspond to the Helbing's original SFM parameter, the up-triangles correspond to the value measured in Ref. [22], squares correspond to zero body force and circles correspond to an extreme value of stiffness (one order of magnitude higher than the original SFM). The down triangles correspond to an intermediate value between the empirical value presented in Ref. [22] and the one provided by Helbing in Ref. [1]

trians.

The existence of the FIF phenomenon for only "stiff" individuals opens many questions on the microscopic dynamics of pedestrians. We may presume that contacts between pedestrians are quite different for soft individuals than for stiff individuals. Thus, we proceed to study the dynamics of contacting pedestrians, regardless of the overlap effects. We will assimilate the pedestrians as nodes and the whole crowd as a network. We will link any two individuals whenever they get in physical contact (*i.e.* $r_{ij} \leq R_{ij}$).

Fig. 2a shows the mean degree of the contact network as a function of the desired velocity. The degree of a node is defined as the number of links that connects this node to any other node. This means, the number of pedestrians that are in physical contact with a given pedestrian. The mean degree is the average of the degree over all the nodes (pedestrians) and over the whole sampled interval. We computed mean values only after the system reached the stationary state, that is, after a well-formed bulk has been established.

Notice that the mean degree increases as v_d increases, as expected. This expresses the fact that higher v_d values accomplish higher densities, forcing individuals to touch each other. For a given v_d, the mean degree reduces as the k_n value increases. A noticeable decrease in the mean degree can be seen for the highest explored value of k_n. This opens the question on how would this affect the sliding friction among pedestrians.

A more detailed insight into the contact dynamics can be acquired from Fig. 2b. The overlap between individuals is shown as a function of v_d. Recall from Section 3.1 that the overlap is defined as $R_{ij} - r_{ij}$ where R_{ij}, is the sum of radius of particle i and particle j and r_{ij} is the distance between both particles. Except for very low desired velocities (say, $v_d < 2\,\mathrm{m/s}$), we can see that the mean overlap is an increasing function of v_d. We will not further analyze the regime $v_d < 2\,\mathrm{m/s}$.

For a given $v_d > 2\,\mathrm{m/s}$, the overlap increases as the k_n value decreases. This can be explained by considering the bulk at a (quasi) equilibrium situation. The social and compression forces counterbalance the desired force. Thus, for any fixed v_d, the product $k_n \times (R_{ij} - r_{ij})$ remains (almost) fixed. Any decrease in k_n allows a more significant intrusion. This (partially) supports the argument that the sliding friction should weaken for stiffer pedestrians (say increasing k_n values).

The sliding friction reduction appears as the first feature for enhancing the overall evacuation performance. Either reducing the mean overlap and the mean degree tend to diminish the mean sliding friction within the crowd. Notice, however, that switching from a FIS regime (positive slope) to a FIF regime (negative slope) in Fig. 1 appears as a more complex phenomenon. We will focus on this issue in an upcoming investigation.

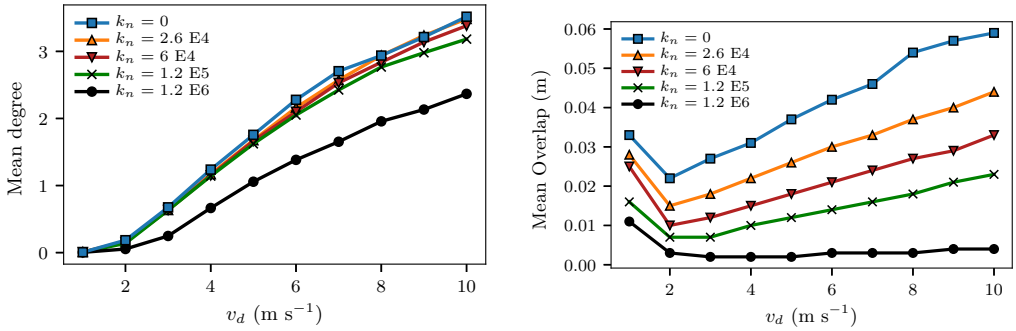

(a) (b)

Figure 2: (a) Mean degree as a function of the pedestrians desired velocity. (b) Mean overlap as a function of the pedestrians desired velocity. Each symbol indicates the k_n value corresponding to the body force (see the labels). The data corresponds to a bottleneck with periodic boundary conditions (re-injecting pedestrians). The average was taken over time and the pedestrians in the bottleneck. The sampling was done every five seconds once the crowd reached the stationary state (say, $t = 20\,\mathrm{s}$) until the end of the simulation ($t = 1000\,\mathrm{s}$). Color online only.

The body force has a notorious impact in the number of pedestrians touching each other (say, the degree). This is clearly depicted in Fig. 3 where four different configurations of the evacuation dynamics are shown. The configurations represent 225 pedestrians trying to escape through a door (see caption for details). The colors correspond to the degree of each node (pedestrian), and the lines between pedestrians represent the contacts among them.

The four configurations corresponds to two different v_d and two different k_n values (say, the minimum and maximum explored values). Fig. 3a and Fig. 3b show snapshots for $k_n = 0$, at the desired velocities of $2\,\mathrm{m/s}$ and $10\,\mathrm{m/s}$, respectively. Fig. 3c and Fig. 3d show similar situations, but for $k_n = 1.2\,\mathrm{E6}$. As expected, increasing the desired velocity compresses the crowd towards the exit.

The four snapshots in Fig. 3 confirm (visually) the fact that more rigid pedestrians ease the crowded environment, widening the occupied region. At $v_d = 10\,\mathrm{m/s}$ (the maximum explored velocity), it can hardly be found pedestrians with degree 6 when $k_n = 1.2\,\mathrm{E6}$, while a lot of them are present for k_n=0.

The clusterization of the pedestrians has a significant impact on the blocking clusters (the group of pedestrians that clog the exit). Fig. 4 shows the blocking cluster probability as a function of the desired velocity for different k_n values (see caption for details). The blocking clusters become more probable for high desired velocity, since the clogged area gets more compact as v_d increases (for any fixed value of k_n). But, the most remarkable fact in Fig. 4 is

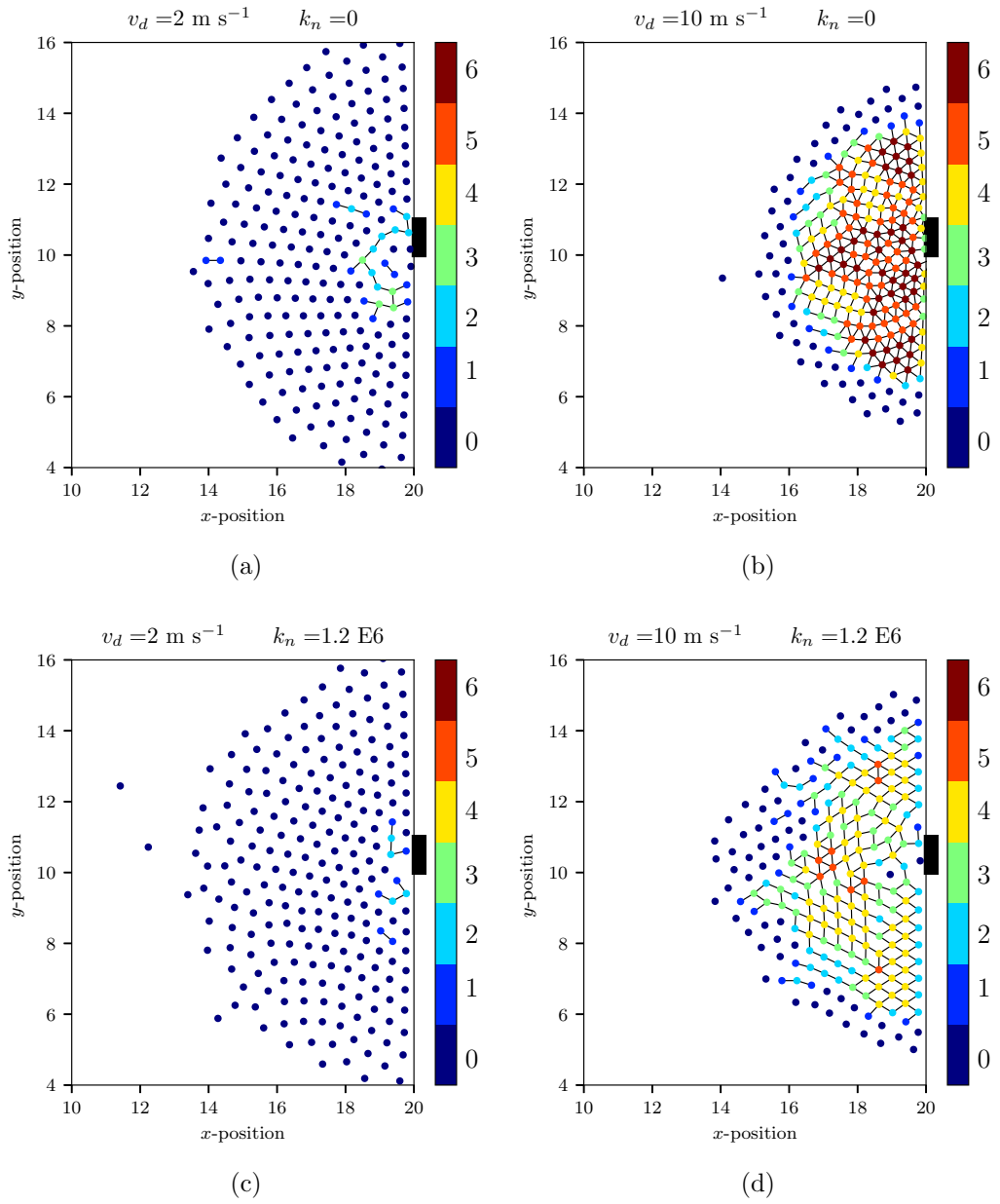

Figure 3: Snapshots of the contact networks of a 225 pedestrian evacuation through a bottleneck. The door is placed at $(x, y) = (20, 10)$ m, the width of the door is 0.92 m (equivalent to 2 pedestrian's diameter). The lines that connect the nodes (pedestrians) represent the contact between them. The color represents the degree (the number of pedestrians with which it is connected). (a) and (b) correspond to a simulation without body force with v_d =2 and v_d =10 respectively. (c) and (d) correspond to simulations with k_n = 1.2 E6 with v_d =2 and v_d =10 respectively. The black rectangle at the right represents the exit door. Color online only.

that increasing the body stiffness reduces the blocking cluster probability for any fixed value of v_d. Recall from Ref. [2] that the evacuation time is controlled by the blocking. Thus, increasing the body stiffness affects the presence of the blocking clusters, and consequently improves the evacuation time. This raises as a second feature for enhancing the overall evacuation performance.

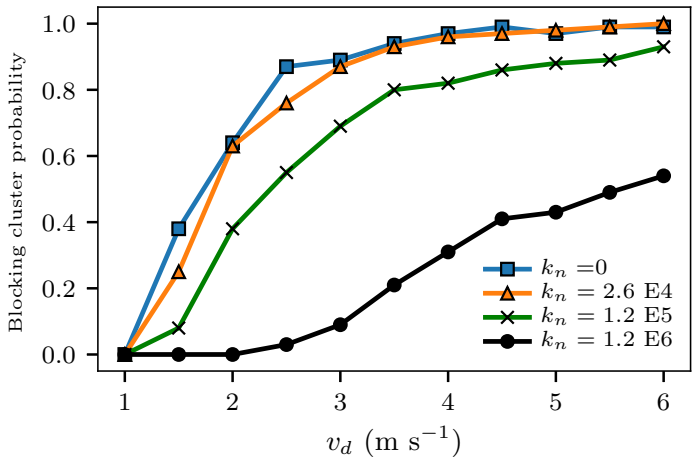

Figure 4: Blocking cluster probability as a function of v_d for different stiffness levels (see label). The probability is calculated as the amount of time a blocking cluster is present divided by the overall simulation time. The situation corresponds to a bottleneck with 225 pedestrians under periodic boundary conditions (re-injection of pedestrians once they left the room). The sampled interval was set to $t_f = 1000\,\mathrm{s}$. Color online only.

We may summarize this Section as follows. Soft pedestrians attain a FIS or FIS+FIF evacuation pattern but, stiff pedestrians exhibit a single FIF pattern. Stiffness affects either the presence of the blocking clusters and the pedestrians overlap. The less they overlap, the less intense becomes the sliding friction among them. Additionally, the fewer the blocking clusters the easier they get out.

4.2 Corridor

We present in this section the results corresponding to the corridor geometry. We first computed the contact network in the same way as in the bottleneck geometry. Fig. 5a shows the mean degree as a function of the global density for different k_n values (see caption for details). The mean degree vanishes at very low densities because the pedestrians do not touch each other. When the density surpasses 4.5, a few pedestrians start to touch each other, raising the mean degree. As the density continuous increasing, the mean degree approaches the asymptotic value of six. Degree six corresponds to the maximum packing density for identical hard disks.

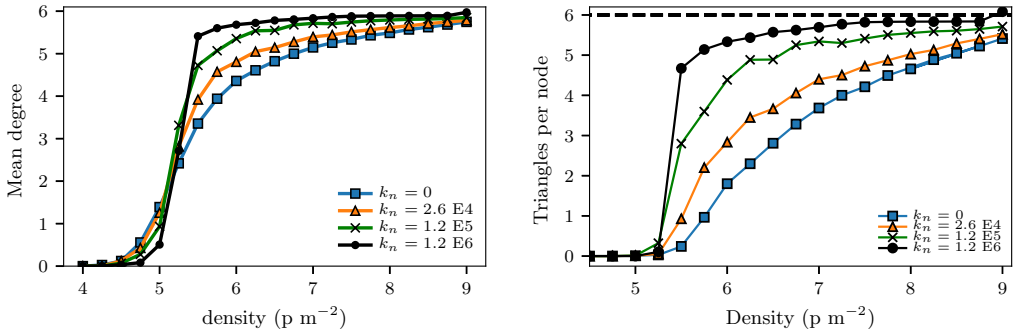

Figure 5: (a) Mean degree as a function of the global density for different k_n values. (b) Triangles per node as a function of the global density. The global density is the total number of pedestrians per unit area. The mean values are averages over all the pedestrians and over time once the system reached the stationary state. The measurements correspond to a corridor of 28 m $\times$ 22 m with periodic boundary conditions and $v_d = 1$. Color online only.

In order to get a better insight on how the pedestrians contact to each other, we present in Fig. 6 two snapshots of the corridor at the stationary situation. Fig. 6a corresponds to $k_n = 0$, while Fig. 6b corresponds to $k_n = 1.2$ E5. The former shows a somewhat disordered network, while the latter exhibits an almost completely ordered lattice. The missing triangles in Fig. 6a are replaced by other polygons of more than three edges.

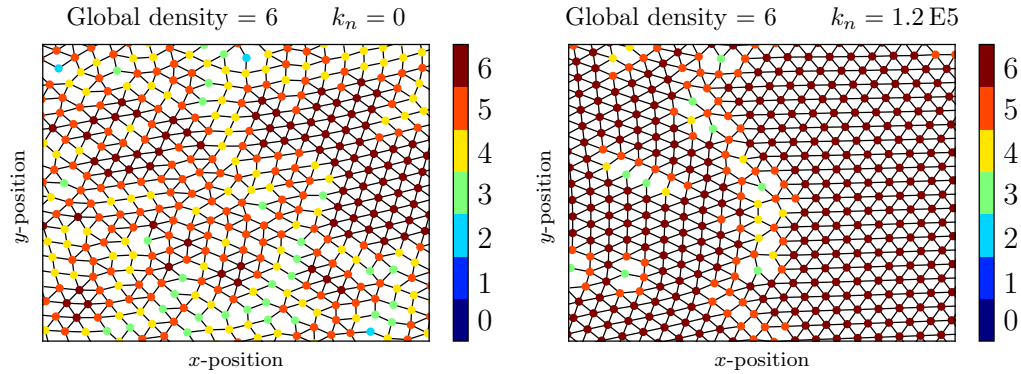

Figure 6: Contact network of the pedestrians along the corridor at time $t = 50$ s. The global density was $\rho = 6$. The lines that connect the nodes (pedestrians) represent the contacts between them. The colors stand for the degree of the node (the number of pedestrians that are in contact with him/her). The corridor was 28 m $\times$ 22 m with periodic boundary conditions and $v_d = 1$. (a) corresponds to a simulation without body force and (b) corresponds to a simulation with $k_n = 1.2$ E5. The friction coefficient and the other SFM parameters are the same as in Section 4.1. Color online only.

We find these topological magnitudes useful for comparing the pedestrian behavior in the corridor geometry with respect to the bottleneck geometry. A re-examination of Fig. 5a (corridor) and Fig. 2a (bottleneck) reveal that the pedestrian stiffness k_n affects differently the way they contact each other. The mean degree increases for "stiff" pedestrians moving along the corridor as the density increased with a sharp increase at $5\,\mathrm{p/m^2}$. Conversely, the mean degree increases for "soft" pedestrians in the bottleneck situation.

Fig. 3 and Fig. 6 illustrate the connectivity differences between the bottleneck and the corridor situation. The bulk in Fig. 3 appears more heavily connected among "soft" pedestrians than among "stiff" pedestrians (see both snapshots at $v_d = 10$). The opposite occurs in Fig. 6. This discrepancy seems to be related to the boundary conditions, since the same SFM parameters were applied on both situations. We may speculate that this phenomenon occurs because, in the corridor, the lateral walls act like a confining barrier that forces the "stiff" pedestrian to increase his (her) contacts. On the contrary, no real confining walls exist in the bottleneck situation (regardless the side walls).

We can test our hypothesis by computing the mean overlap. Fig. 7 shows this magnitude for the corridor situation. Notice that "soft" pedestrians attain more overlap than the "stiff" ones, as expected. This is in agreement with Fig. 2b for the bottleneck situation (at a fixed value of v_d). The curves in Fig. 2b, however, do not meet each other as in Fig. 7 where all the curves meet each other at high-density values. This phenomenon occurs due to space limitations in the corridor that produces overlapping (almost) independently of the value of k_n.

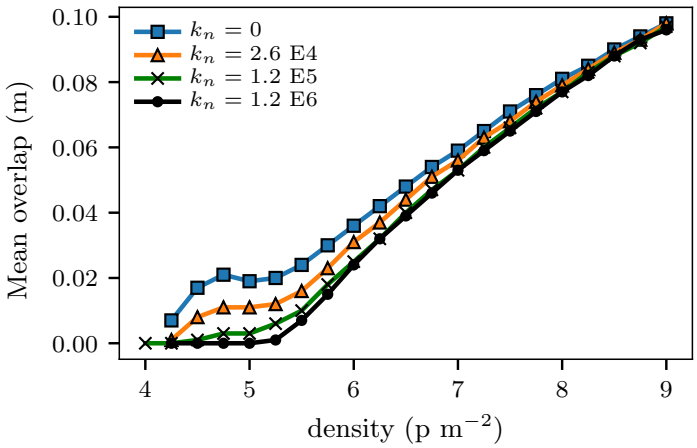

Figure 7: Mean overlap as a function of the global density. The global density is the total number of pedestrians per unit area. The mean values are averages over all the pedestrians and over time once the system reached the stationary state. Both measurements correspond to the corridor geometry with desired velocity $v_d = 1$. Color online only.

The above results represent an important step in the investigation. The inter-pedestrian connectivity differences between the bottleneck geometry and the corridor geometry were not expected and opens two major questions: how do the pedestrians interact with the walls as a function of the body stiffness, and consequently, how does this affect the flux across the corridor.

We start by computing the mean velocity across the corridor. Fig. 8 shows the mean velocity $\langle v_x \rangle$ (parallel to the corridor) as a function of the stiffness for different global density levels. This plot shows a flat pattern for $k_n < 10^4$ and a slowing down above this threshold. This is opposed to what happens in the bottleneck geometry (not shown).

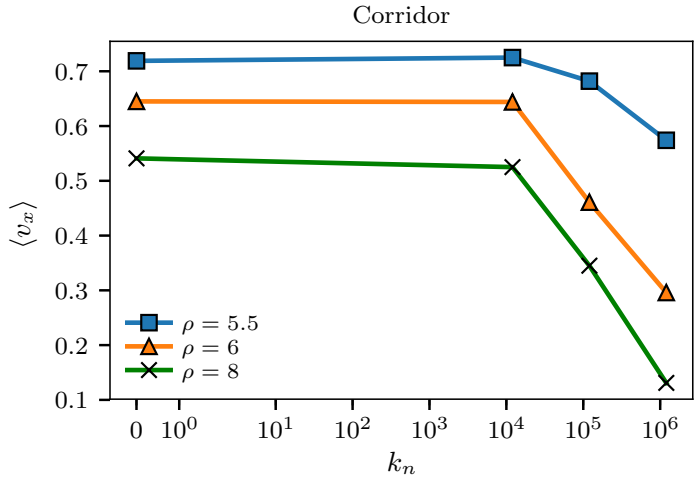

Figure 8: Mean velocity in the longitudinal coordinate (v_x) as a function of the stiffness k_n for three different global densities (see label in the plot). The measurements correspond to a corridor of 28 m $\times$ 22 m with periodic boundary conditions and $v_d = 1$. The average was taken along the corridor and along the simulated time. Color online only.

The $\langle v_x \rangle$ values in Fig. 8 were computed at densities $\rho \geq 5.5$. According to Fig. 7, at these densities, the overlaps among pedestrians attain significant values. Furthermore, stiffness values $k_n \geq 10^4$ move the system to a more heavily connected stage, and thus, pedestrians have no choice but to walk at (almost) the same speed as his (her) neighbors. This behavior may be envisaged as the passage from a "free" walking movement to a constrained walking movement as the stiffness increases. A more physical picture would assimilate the former as a "fluid-like state" and the latter as a "solid-like state". When the stiffness is very high (say k_n =1.2 E6), all the pedestrians are expected to walk at a common velocity. The pedestrians that walk in physical contact with the wall are the ones who determine the velocity of the whole crowd, as discussed below.

Fig. 9a shows the velocity profile ($\langle v_x \rangle$ vs. the transversal coordinate y)

for different k_n values. For $k_n = 0$, we can see a parabolic-like velocity profile which means that the friction with the walls reduces the speed of pedestrians. The velocity profile resembles the Poiseuille flow (similar to Newtonian and incompressible fluids in a laminar regime). This behavior was also observed in empirical measurements of crowd dynamics reported in Ref. [23]. But as k_n increases the velocity profile flattens until becoming (almost) uniform (see Fig. 9a for $k_n = 1.2\,\mathrm{E6}$). In this scenario, v_x attains a much lower value than in the case of soft pedestrians (k_n =0).

From the results displayed above, we realize that the crowd behaves like a solid for very stiff pedestrians. This means that the crowd can not be easily "deformed". In this context, deformation means that some parts of the crowd may be allowed to move faster than other parts of the crowd.

The strain rate tensor displays the rate of change of the deformation of a body in the vicinity of a given point. We consider the following discrete definition of the strain rate:

$$\dot{\gamma} = \frac{\langle v_x(\text{center})\rangle - \langle v_x(\text{boundary})\rangle}{|y(\text{center}) - y(\text{boundary})|} \tag{6}$$

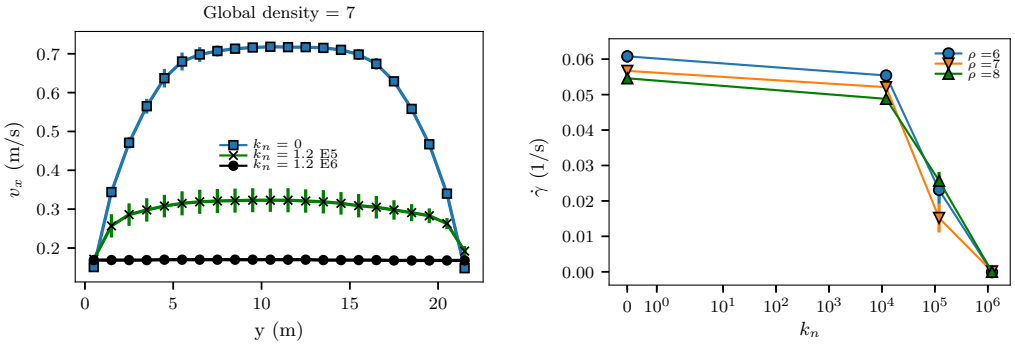

(a) (b)

Figure 9: (a) Mean velocity in the x coordinate as a function of the transversal coordinate y for three different stiffness values k_n (see the label). (b) Strain rate as a function of the stiffness level k_n for three different global density values (see label). Data correspond to a corridor of $28\,\mathrm{m} \times 22\,\mathrm{m}$ with periodic boundary conditions and $v_d = 1$. The global density was $\rho = 7p\,\mathrm{m}^{-2}$. Color online only.

Where $\langle\cdot\rangle$ means the average taken over time. This definition compares the velocity of the pedestrians close to the wall (boundary) with respect to the velocity of the pedestrians at the center of the corridor (center). Thus, the strain rate $\dot{\gamma}$ vanishes (no deformation) as the stiffness level increases. This phenomenon is shown in Fig. 9b where we can see that the strain rate drops for high values of k_n.

We conclude this Section by stressing, once again, that stiffer pedestrians attain opposite results in corridors with respect to bottlenecks. The walls in the corridors play a critical role that prevents pedestrians from detaching from each other. This effect can be observed as an increment in the connectivity of the contact network and the flattening of the velocity profile (thus reducing the strain rate). High enough stiffness values stuck the pedestrians leading to a "solidification" of the crowd. All the pedestrians walk at almost the same velocity at this stage. The pedestrians that are in contact with the walls are the ones that determine the velocity of the whole crowd. We already analyzed this situation in Ref [24].

4.3 Dimensionless numbers and comparison with empirical data

We consider the empirical measurements from Ref. [8] corresponding to the fundamental diagram obtained at the entrance of the Jamaraat bridge (see the inset in Fig. 10a). Our aim is to reproduce the qualitative behavior of these measurements.

Figs. 10 show the pedestrian flow as a function of the global density (fundamental diagram). Fig. 10a corresponds to $k_n = 0$ (this is *i.e.* $k_n = 0$) while Fig. 10b corresponds to $k_n = 1.2\,\mathrm{E}5$. Each curve represents different friction values (see the caption for details).

According to the empirical measurements at Jamaraat, the flow slows down for high enough densities due to jamming. Notice that the original SFM (corresponding to $k_t = 2.4\,\mathrm{E}5$) does not produce the expected slowing down for null body force ($k_n = 0$). However, when the body force is present (the original SFM) an "U" shape behavior occurs for densities above 5 p^{-2}.

The increase in k_t to $k_t = 1.2\,\mathrm{E}6$ (five times the original SFM value) slows down the flux for densities above 5 p m^{-2}, regardless of the presence of the body force. Including the body force, however, produces a subtle increment in the flow for densities higher than 7 p m^{-2} (see orange curve from Fig. 10a).

A further increment of k_t to $k_t = 2.4\,\mathrm{E}6$ (ten times the original SFM value) attains a plateau ($\rho > 5$ p m^{-2}) before vanishing at very high densities. This occurs on either $k_n = 0$ and $k_n = 1.2\,\mathrm{E}5$.

These results suggest that although increasing k_n slows down the flux, it is still necessary to increase the friction coefficient k_t to avoid an "U" shape behavior for extremely high densities.

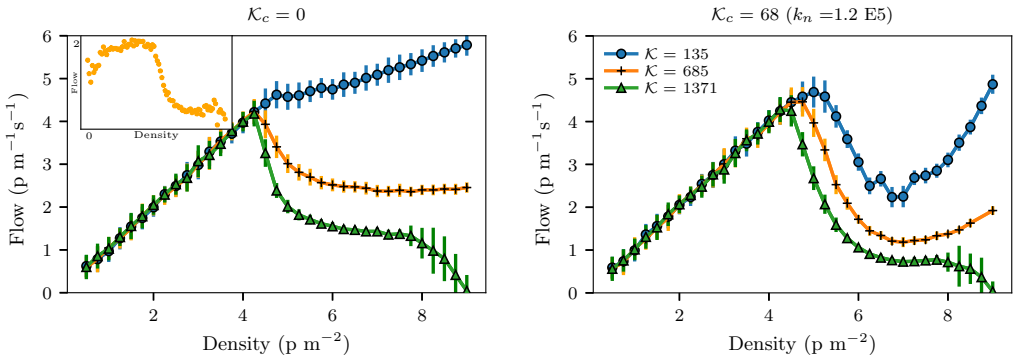

(a) (b)

Figure 10: Flow vs. global density. The flow is calculated in a circular area of $R = 1\,\mathrm{m}$ at the center of the corridor. The circular markers correspond to the original friction of the SFM, the "+" symbol corresponds to the friction increased by a factor of five and the triangles correspond to the friction increased by a factor of ten. The desired velocity was $v_d = 1$ in all the cases. (a) corresponds to simulations without body force (k_n =0) and (b) corresponds to a body force with the original value of the body stiffness ($k_n = 1.2\,\mathrm{E5}$). Color online only.

5. Conclusions

We explored the effect on the pedestrians dynamics of the (sometimes neglected) body force in the framework of the SFM. We showed that the stiffness coefficient (k_n) has a significant impact on the evacuation dynamics (bottleneck) and also in the dynamics of pedestrians walking along a straight corridor.

In the bottleneck geometry, the evacuation time diminishes (pedestrians move faster) as pedestrians become stiffer along the explored desired velocities. This phenomenon occurs because stiffer pedestrians reduce the overlapping and hence the sliding friction intensity. This scenario releases more easily the pedestrians and reduces the probability of producing a cluster of pedestrians blocking the exit (blocking cluster). This leads to a more efficient evacuation dynamics.

The opposite behavior is obtained in the corridor geometry with respect to the bottleneck geometry. The major difference is that pedestrians are limited to the available space between walls in the corridor geometry. Thus, the overlap between pedestrians is controlled by the available space. But, stiffer pedestrians are more likely to get stuck. The whole crowd can be compared to a granular material. Granular materials can be disordered (amorphous) or ordered depending on how particles interact with each other. In the present context, at low stiffness levels, the crowd appears disordered attaining a parabolic velocity profile. If the stiffness level is high, the whole crowd appears ordered into a lattice (like a crystalline solid) with a uniform velocity profile that depends on the friction interaction with the walls.

Our efforts to "tune" the original SFM to reproduce empirical data (say, the fundamental diagram) moved us to explore the dimensionless parameter space. We found that we can qualitatively reproduce the empirical data if the parameters are close to $k_n < 1.2\,\mathrm{E}5$ and $k_t = 1.2\,\mathrm{E}6$.

Acknowledgments

This work was supported by the National Scientific and Technical Research Council (spanish: Consejo Nacional de Investigaciones Científicas y Técnicas - CONICET, Argentina) grant Programación Científica 2018 (UBACYT) Number 20020170100628BA.

G. Frank thanks Universidad Tecnolólica Nacional (UTN) for partial support through Grant PID Number SIUTNBA0006595.

References

[1] D. Helbing, I. Farkas, and T. Vicsek. Simulating dynamical features of escape panic. Nature, 407:487–490, 2000.

[2] D. Parisi and C. Dorso. Microscopic dynamics of pedestrian evacuation. Physica A, 354:606–618, 2005.

[3] D. Parisi and C. Dorso. Morphological and dynamical aspects of the room evacuation process. Physica A, 385:343–355, 2007.

[4] G. Frank and C. Dorso. Room evacuation in the presence of an obstacle. Physica A, 390:2135–2145, 2011.

[5] Taras I. Lakoba, D. J. Kaup, and Neal M. Finkelstein. Modifications of the helbing-molnr-farkas-vicsek social force model for pedestrian evolution. SIMULATION, 81(5):339–352, 2005.

[6] Paul A. Langston, Robert Masling, and Basel N. Asmar. Crowd dynamics discrete element multi-circle model. Safety Science, 44(5):395 – 417, 2006.

[7] Peng Lin, Jian Ma, You-Ling Si, Fan-Yu Wu, Guo-Yuan Wang, and Jian-Yu Wang. A numerical study of contact force in competitive evacuation. Chinese Physics B, 26(10):104501, sep 2017.

[8] Dirk Helbing, Anders Johansson, and Habib Zein Al-Abideen. Dynamics of crowd disasters: An empirical study. Phys. Rev. E, 75:046109, Apr 2007.

[9] I. M. Sticco, F. E. Cornes, G. A. Frank, and C. O. Dorso. Beyond the faster-is-slower effect. Phys. Rev. E, 96:052303, Nov 2017.

[10] Rainald Lohner, Britto Muhamad, Prabhu Dambalmath, and Eberhard Haug. Fundamental diagrams for specific very high density crowds. Collective Dynamics, 2, 2018.

[11] Dirk Helbing and Péter Molnár. Social force model for pedestrian dynamics. Phys. Rev. E, 51:4282–4286, May 1995.

[12] Anders Johansson. Constant-net-time headway as a key mechanism behind pedestrian flow dynamics. Phys. Rev. E, 80:026120, Aug 2009.

[13] Meifang Li, Yongxiang Zhao, Lerong He, Wenxiao Chen, and Xianfeng Xu. The parameter calibration and optimization of social force model for the real-life 2013 yaan earthquake evacuation in china. Safety Science, 79:243 – 253, 2015.

[14] S.P. Hoogendoorn and W. Daamen. Microscopic Calibration and Validation of Pedestrian Models: Cross-Comparison of Models Using Experimental Data. In A. Schadschneider, T. Pöschel, R. Kühne, M. Schreckenberg, and D. E. Wolf, editors, Traffic and granular flow '05, volume Part III. Springer, 2007.

[15] A. Seyfried, B. Steffen, W. Klingsch, Th. Lippert, and M. Boltes. The Fundamental Diagram of Pedestrian Movement Revisited - Empirical Results and Modelling. In A. Schadschneider, T. Pöschel, R. Kühne, M. Schreckenberg, and D. E. Wolf, editors, Traffic and granular flow '05, volume Part III. Springer, 2007.

[16] A. Johansson, D. Helbing, and P.K. Shukla. Specification of the social force pedestrian model by evolutionary adjustment to video tracking data. Advances in Complex Systems, 10(supp02):271–288, 2007.

[17] Mehdi Moussaï d, Dirk Helbing, Simon Garnier, Anders Johansson, Maud Combe, and Guy Theraulaz. Experimental study of the behavioural mechanisms underlying self-organization in human crowds. Proceedings of the Royal Society B: Biological Sciences, 276(1668):2755–2762, 2009.

[18] M. Luber, J. A. Stork, G. D. Tipaldi, and K. O. Arras. People tracking with human motion predictions from social forces. In 2010 IEEE International Conference on Robotics and Automation, pages 464–469, May 2010.

[19] Stefan Seer, Christian Rudloff, Thomas Matyus, and Norbert Brändle. Validating social force based models with comprehensive real world motion data. Transportation Research Procedia, 2:724 – 732, 2014. The Conference on Pedestrian and Evacuation Dynamics 2014 (PED 2014), 22-24 October 2014, Delft, The Netherlands.

[20] Ulrich Weidmann. Transporttechnik der fussgänger. IVT Schriftenreihe, 90, Jan 1992.

[21] J. Song, F. Chen, Y. Zhu, N. Zhang, W. Liu, and K. Du. Experiment calibrated simulation modeling of crowding forces in high density crowd. IEEE Access, 7:100162–100173, 2019.

[22] John W Melvin. Aatd system technical characteristics, design concepts, and trauma assessment criteria. task ef final report. Technical report, 1988.

[23] XL Zhang, WG Weng, HY Yuan, and JG Chen. Empirical study of a unidirectional dense crowd during a real mass event. Physica A: Statistical Mechanics and its Applications, 392(12):2781–2791, 2013.

[24] I.M. Sticco, G.A. Frank, F.E. Cornes, and C.O. Dorso. A re-examination of the role of friction in the original social force model. Safety Science, 121:42 – 53, 2020.